

Insufficient data across many regions of Canada renders categorizing geothermal resources a difficult task. As a result, computer modelling coupled with laboratory investigations to fill data gaps are being encouraged under the Executive Summary, Research Needs of the Geological Survey of Canada Open File 6914 [5]. The warm sedimentary Williston Basin extending from the south of the Province of Saskatchewan is the area that has been of prime interest for geothermal exploitation. Therefore, the paper presents detailed thermal investigations into this area and highlights a potential production field region. Figure 1 indicates the location and number of wells used to perform these investigations.

2. Heat Flow and Subsurface Temperature Estimations

The bottom-hole temperatures (BHTs) obtained from the geological well data should be corrected. This correction is seen in Figure 2 through the linear trendline of the corrected well data. BHT data are usually of low quality as mentioned by Blackwell [3, 4] and Shope [10]. The true formation temperature values are not represented by the geophysical logs. This is because of recording the data shortly after cessation

of drilling operation.

The Harrison correction can be described as a second order polynomial function of depth. Through this method the generated ΔT value in $^{\circ}\text{C}$ is a correction factor that is summed to the BHT from the geological well data to yield corrected well data temperature. It is stated by the following:

$$\Delta T(^{\circ}\text{C}) = -16.51 + 0.01827z - 2.345 \times 10^{-6}z^2 \quad (1)$$

The True Vertical Depth (TVD) is given by z in Eq. (1). It can be noted through the application of the Harrison correction method to the uncorrected trendline, the R^2 value increases by approximately 0.1 (this accounts for a greater correlation between the temperature and depth values).

As outlined by Grasby [5] from the Open file 6914 report on Geological survey of Canada, areas of the WCSB displaying known temperatures between $80^{\circ}\text{C} - 150^{\circ}\text{C}$ are regions of potential binary systems. Therefore, for a geothermal reservoir exhibiting medium-temperature above 80°C , electricity can still be generated by means of a binary cycle power plant.

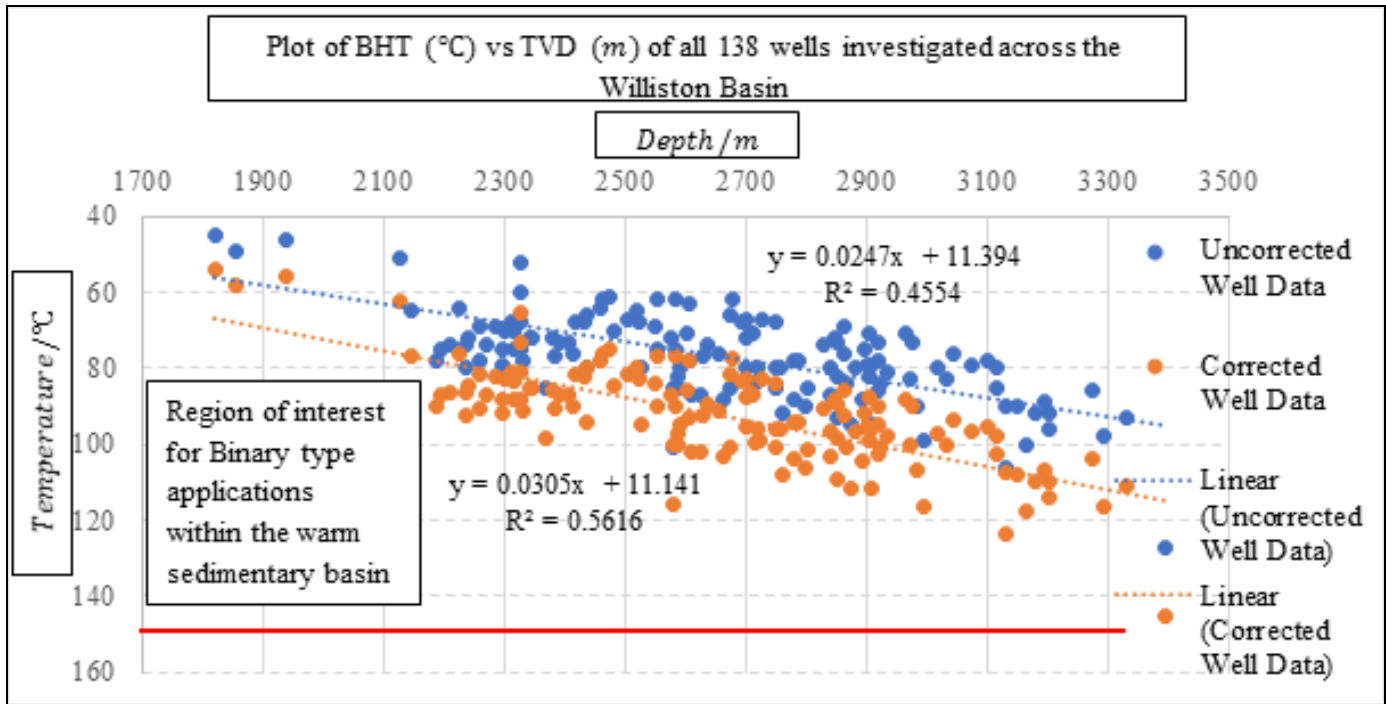


Fig 2: Graphical representation of corrected well data highlighting the potential exploitable region of $80^{\circ}\text{C} - 150^{\circ}\text{C}$ within the Williston Basin.

2.1 Thermal Gradient Findings

The thermal gradient for each well is calculated utilizing the corrected well data. The thermal gradient is calculated as:

$$\left(\frac{dT}{dz}\right) = \frac{T_{BHT} - T_s}{z} \quad (2)$$

where dT/dz is the thermal gradient, T_{BHT} is the corrected

BHT values, T_s is the average annual surface temperature, and z is the true vertical depth. All temperature values are calculated in degree Celsius ($^{\circ}\text{C}$), and the TVD in meters (m). The average thermal gradient for the investigated region of the Williston Basin was determined to be $34.01^{\circ}\text{C}/\text{km}$. For the regions across the Williston Basin (south of the Province Saskatchewan) an average annual surface temperature, T_s of 2°C is used in the calculation of the thermal gradients [2].

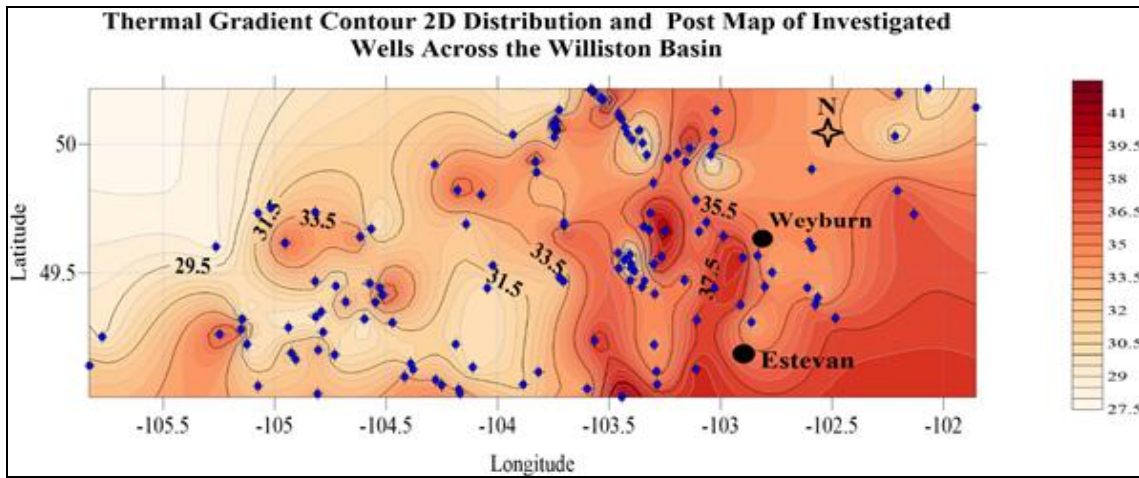


Fig 3: Map of Thermal Gradient showing all 138 wells across the Williston Basin.

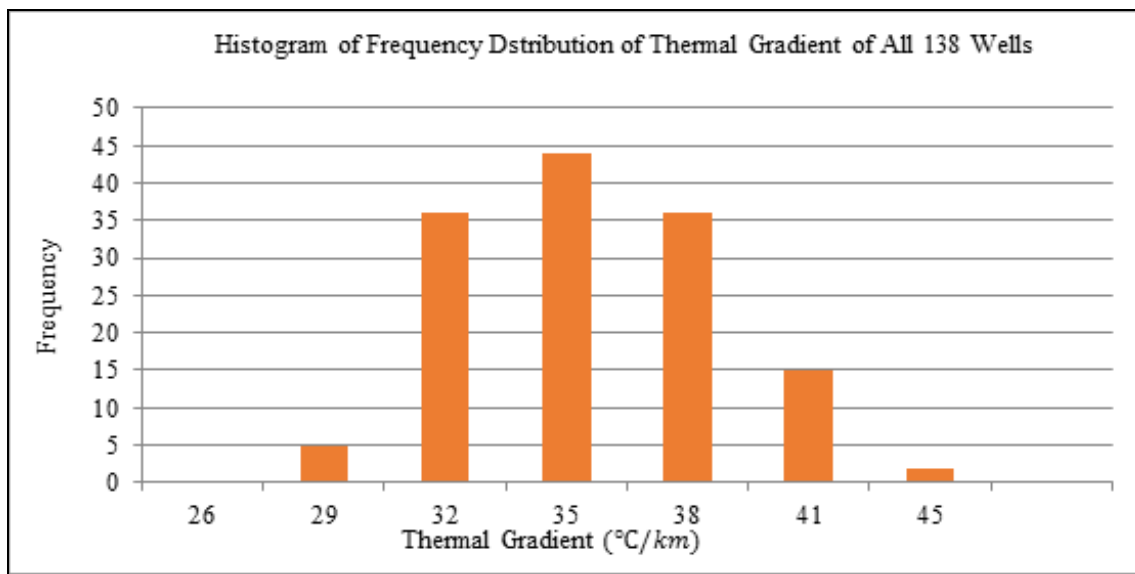


Fig 4: Frequency distribution of thermal gradient values across the Williston Basin.

Through the 2D contour distribution map of Fig 3, areas of thermal gradient values greater than 34.01 °C/km, are highlighted within the proximity of both Weyburn and Estevan. In addition, the distribution of the data points (this is indicated by the post map) will have a greater accuracy within the coordinates 49 °N – 50 °N latitude and 102 °W – 104 °W longitude. Within this area the data point density is the highest, hence the Kriging method utilized by the Surfer 14 software will yield better results also within this area. Finally, it can be noted from the histogram of Fig 4, the distribution of thermal gradient values are nearly that of a standard normal distribution curve, having a skewness of about 0.276 (skewed to the right; right tail is longer than the left tail). This skewed right tail is reflected by a kurtosis value of about -0.286 (hence “light tailed” distribution).

2.2 Surface Heat Flow

The surface heat flow is then calculated from the corrected thermal gradient values. A 1D vertical conduction of heat through the rock column can be assumed; hence the resulting

heat flow can be expressed as:

$$Q_s = k \left(\frac{dT}{dz} \right) \tag{3}$$

where the corrected thermal gradient is in °C/km, the thermal conductivity *k*, is in W/mK, and the calculated heat flow *Q_s*, is in mW/m².

For the 1D case to be accurate the following conditions must hold to prevent the nullification of the assumption of steady-state heat flow: the depth of the well is small compared to the distance of significant structural alterations in geology, and excluding current volcanism within the area [11].

The thermal conductivity of the dominant lithology found in each well number was compiled across multiple sources of literature [1, 7, 8]. These formations are comprised of Black Island, Deadwood, Precambrian, Winnipeg and Yeoman. The dominant lithology of these formations comprised of sandstone, shale, igneous rock, gneiss and quartz. Therefore, the thermal conductivity *k* (W/mK) values were the key

component in affecting the surface heat flow values. This is seen when comparing Figures 3 and 5, as areas of high thermal

gradient which do not translate directly into areas of high surface heat flow.

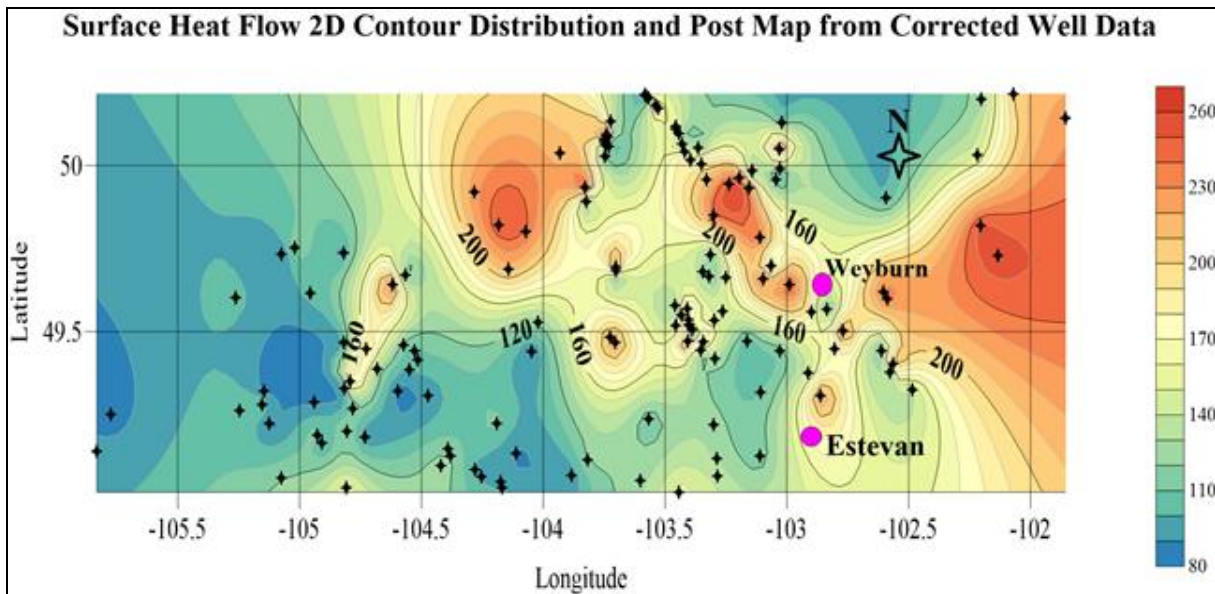


Fig 5: Surface heat flow map with well distribution

2.3 Subsurface Heat Flow Findings

Based on Fig 2, it is observed that the data points range from around 1800 m – 3300 m. However, the data points have the highest density within the range 2200 m – 2900 m, as this should be taken into consideration for the reliability of such a plot. Therefore, to determine subsurface temperatures, T_z , (z is the depth) at depths 2.5 km, 3.0 km and 3.5 km, heat flow maps can be utilized for these calculations. Through the ‘Lachenbruch model’ which describes the exponential decrease of crustal heat generation with depth, the calculations to determine the variation of temperature with depth are possible. The basement heat flow, Q_0 (W/m^2) is statistically correlated to the heat generation of the basement, A_0 (W/m^3) in the form:

$$Q_0 = Q_r + DA_0 \tag{4}$$

where Q_r is the reduced heat flow (W/m^2) and D is measured in units of depth. Furthermore both Q_r and D are constants characteristic of large geological provinces.

The key parameters used to calculate temperature with depth relations for the geological Craton region are [5]: $D = 9.6$ km, $Q_r = 33$ mW/m², and $A_0 = 2.7$ μW/m³. The basement heat flow value will be the same for all wells under investigation, as this value was found to be 58.92 mW/m². Through a Phanerozoic isopach map by Majorowicz [6] it is observed that within Canada a depth of 3.5 km is reached at the base of the sedimentary section of Williston Basin.

Given that the basin fill of 2 km is overlying the basement at depth of 3.5 km, the temperature $T_{2\text{ km}}$ at the top of the basement needs to be found first.

Therefore at $X = (0 - 2)$ km.

$$T_{2\text{ km}} = \frac{Q_0 X}{k} - A_0 \frac{X^2}{k} \tag{5}$$

For $X > 2$ km, the temperature (T) vs. depth (m) equation can be written as:

$$T(z) = T_{2\text{ km}} + Q_r \frac{z}{k} + \frac{A_0 D^2 [1 - \exp(-\frac{z}{D})]}{k} \tag{6}$$

Equations (5) and (6) explicitly allows the calculation of the subsurface temperatures $T_{2.5\text{ km}}$, $T_{3.0\text{ km}}$, and $T_{3.5\text{ km}}$. Figure 6 parts (a), (b) and (c) were all generated using the Surfer 14 software for depths of 2.5 km, 3.0 km and 3.5 km respectively.

It can be observed that the subsurface temperatures for the wells within the coordinate ranges of (103.75° – 105.25°) W and (49.0° – 49.5°) N are consistent. This region of interest steadily holds and increase in subsurface temperature moving from depth 2.5 km to 3.5 km. In addition, it can be noted that a greater number of well data points exist within this region (having a high data point density for a stronger correspondence between averaging temperature values). Although the wells highlighted by the oval in Fig 6-part c, are among the highest thermal gradient values (refer to Fig 2), these wells are not positioned within an overall region of high subsurface values. These few wells are isolated (lower data point density leading to a weaker estimation of subsurface temperatures). As a result, the main finding of this investigation can indicate that the wells within the area of interest (black rectangle in Fig 6-part c), can be considered as a possible production field for geothermal exploitation.

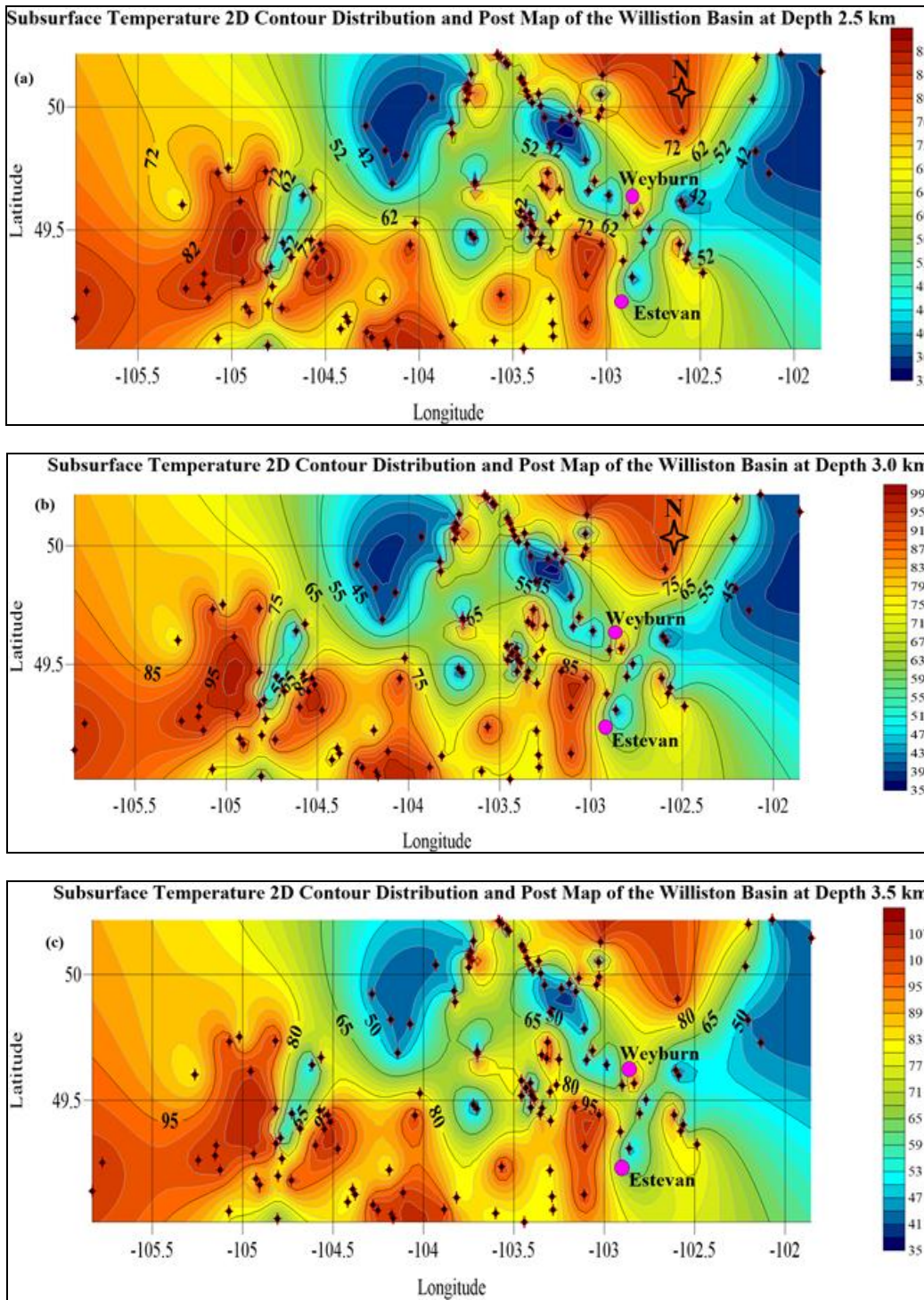


Fig 6: Subsurface Temperatures, $T(z)$:(a) 2.5 km, (b) 3.0 km, (c) 3.5 km

3. Conclusion and Future Work

The subsurface temperatures findings for $T_{2.5\text{ km}}$, $T_{3.0\text{ km}}$, and $T_{3.5\text{ km}}$ all clearly point towards a potential production field left of Estevan. This region lies within the coordinate ranges of $(103.75^\circ - 105.25^\circ)W$ and $(49.0^\circ - 49.5^\circ)N$. These values are within the $80\text{ }^\circ\text{C} - 150\text{ }^\circ\text{C}$ range for binary type geothermal plant application. The integration of hydraulic parameters into the contour maps can yield a greater insight into flow field across the production region (for identification of possible

injection and production wells). Furthermore, calculations and computer simulations of well spacing for plant and reservoir lifetimes can be performed within the area of interest.

4. Acknowledgments

Special mention must be given to the academic staff and postgraduate members at the University of Saskatchewan (UofS), Department of Civil & Geological Engineering, Saskatchewan, Canada. Their assistance was important in accessing geological well core logs from IHS AccuMap

(AccuLogs). The geological logs are accessed through <https://www.ihc.com/products/oil-gas-tools-accumap.html>.

5. References

1. Barker C. Thermal Modeling of Petroleum Generation: Theory and Applications. In: Developments in petroleum science, Elsevier, Amsterdam, 1996; 45:512.
2. Beltrami Hugo. Ground surface temperatures in Canada: Spatial and temporal variability. *Geophysical Research Letters*, doi: 10.1029/2003GLO17144, 2003; 30(10):1499.
3. Blackwell DD, Negraru PT, Richards MC. Assessment of the Enhanced Geothermal System Resource Base of the United States, Natural Resource Research, 2007-2006, 283-308.
4. Blackwell DD, Batir J, Frone Z, Park J, Richards M. New geothermal resource map of the northeastern US and technique for mapping temperature at depth. *GRC Transactions*, 2010, 34. Document ID 28663.
5. Grasby SE, Allen DM, Bell S, Chen Z, Ferguson G, Jessop A, *et al.* Kelman M, Ko M, Majorowicz J, Moore M, Raymond J, Therrien R. Geothermal Energy Resource Potential of Canada. Geological survey of Canada open file 6914, 2012.
6. Majorowicz JA, Jones FW, Jessop AM. Geothermics of the Williston Basin in Canada in Relation to Hydrodynamics and Hydrocarbon Occurrences. *Geophysics*. 1986; 51:767-779.
7. Reiter M, Jessop AM. Estimates of Terrestrial Heat Flow in Offshore Eastern Canada. *Can. J. Earth Sci.*, 1985; 22:1503-1517.
8. Reiter M, Tovar RJC. Estimates of Terrestrial Heat Flow in Northern Chihuahua, Mexico, based upon petroleum bottom hole temperatures. *Geological Society of American Bulletin*, 1982; 93:613-624.
9. Sanyal SK. Future of Geothermal Energy. Proceedings the Thirty-Fifth Workshop on Geothermal Reservoir Engineering, Stanford University, 2010, SGP-TR-188.
10. Shope EN, Reber TJ, Stutz GR, Aguirre GA, Jordan TE, Tester JW. *Et al.* Geothermal Resource Assessment: A Detailed Approach to Low-Grade Resources in the State of New York and Pennsylvania, 37th Stanford Geothermal Workshop, Stanford, CA, 2012, 1.
11. Stutz GR, Williams M, Frone Z, Reber TJ, Blackwell D, Jordan T, *et al.* Tester JW. A Well by Well Method for Estimating Surface Heat Flow for Regional Geothermal Resource Assessment. Proceedings the Thirty-Seventh Workshop on Geothermal Reservoir Engineering, Stanford University, 2012, SGP-TR-194.